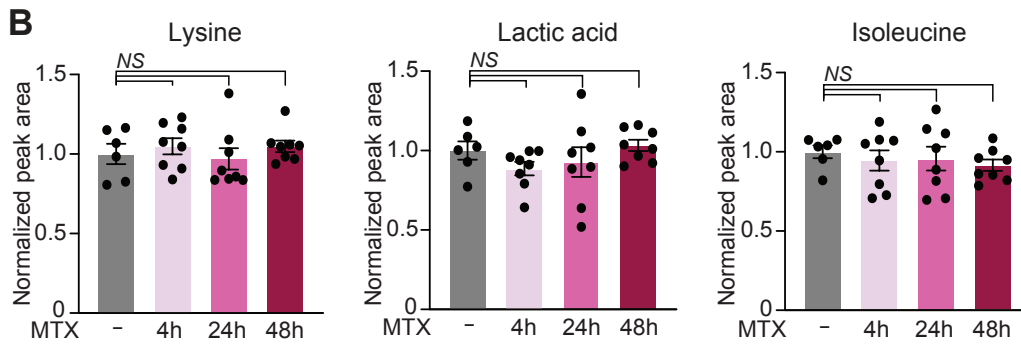
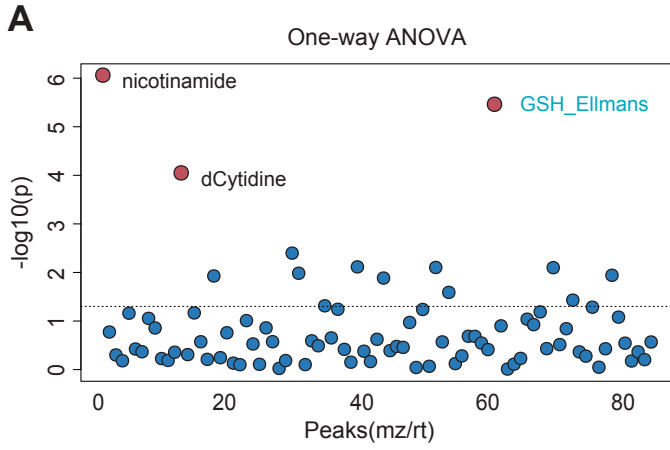


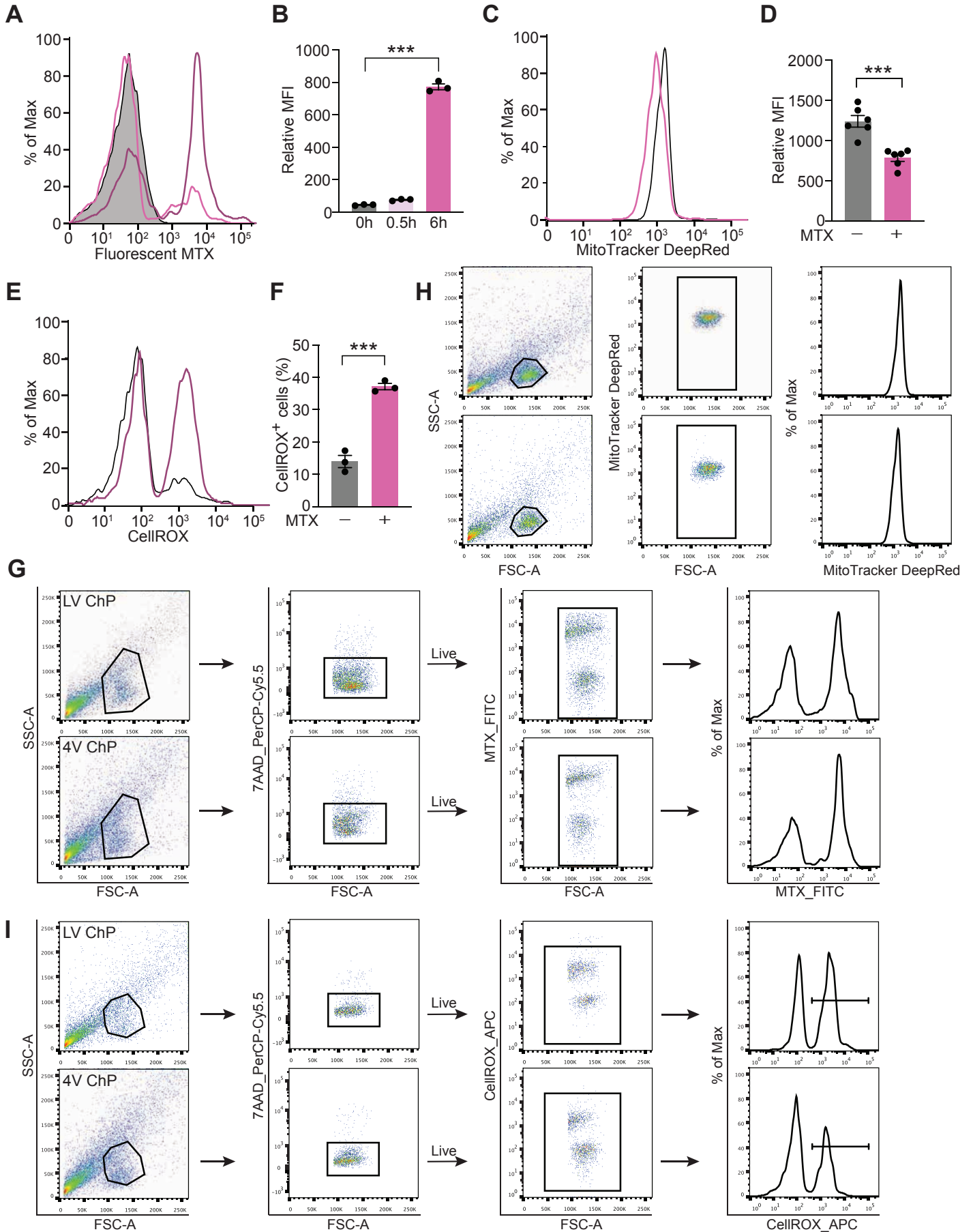
# Supplemental Figure S1



**Supplemental Figure S1. CSF of MTX-treated mice is metabolically altered and presents markers of oxidative stress, Related to Figure 1.** (A) One-way ANOVA of metabolic changes in mouse CSF in response to MTX treatment. Vehicle- and MTX-treated CSF samples were compared at 4 h, 24 h and 48 h following MTX treatment. Significantly changed metabolites are indicated. (B) Levels of amino acids at indicated time points following MTX delivery. NS, not significant. Data represent mean  $\pm$  SEM.

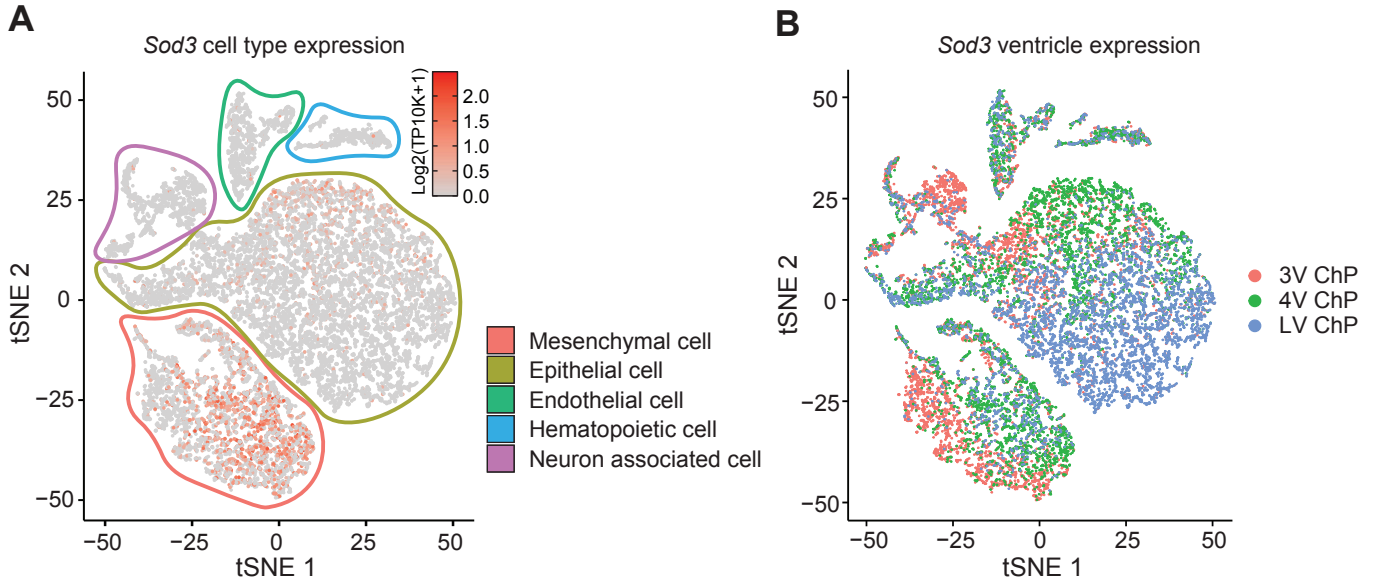
Supplemental Figure S2

Jang et al.



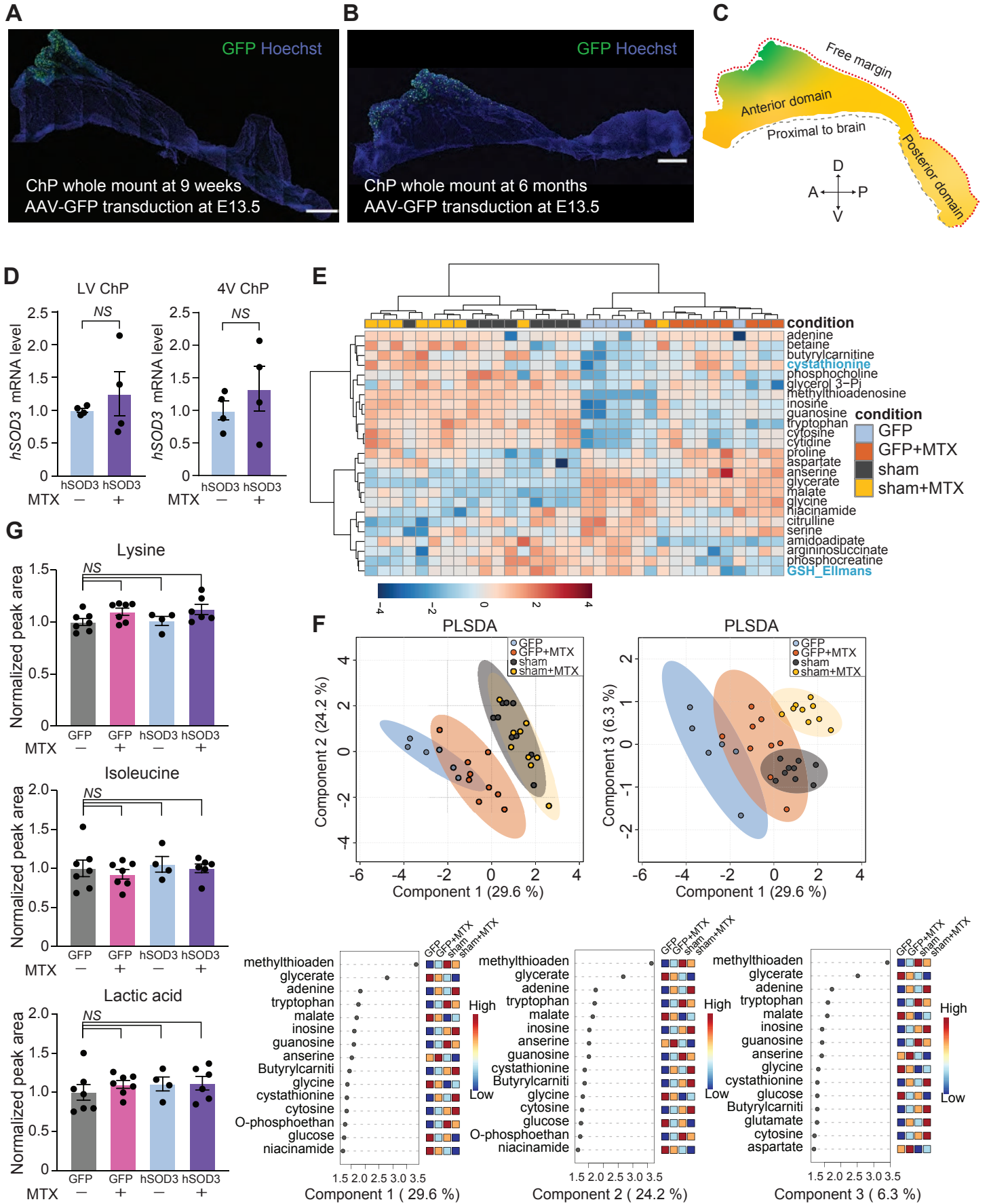
**Supplemental Figure S2. 4V ChP, like LV ChP, is vulnerable to MTX-mediated oxidative stress, Related to Figure 2.** (A, B) Flow cytometry analysis of cells from mouse 4V ChP following incubation with 2  $\mu$ M fluorescent MTX at designated time points. Representative histogram (A) and mean fluorescence intensity (MFI) of fluorescent MTX (B) are shown.  $n = 3$  per group.  $***P < 0.001$ . One-way ANOVA with Tukey's post hoc test. Data represent mean  $\pm$  SEM. (C, D) MitoTracker Deep Red staining of mouse 4V ChP following treatment with vehicle or 10  $\mu$ M MTX for 2 h. Results were analyzed by flow cytometry. Representative histogram (C) and mean fluorescence intensity (MFI) of the MitoTracker Deep Red signal (D) are shown.  $n = 6$  per group.  $***P < 0.001$ . Unpaired  $t$  test. Data represent mean  $\pm$  SEM. (E, F) ROS were assessed by CellROX staining in mouse 4V ChP following incubation with vehicle or 10  $\mu$ M MTX for 4 h. Results were analyzed by flow cytometry. Representative histogram (E) and the percent CellROX<sup>+</sup> cells (F) are shown.  $n = 3$  per group.  $***P < 0.001$ . Unpaired  $t$  test. Data represent mean  $\pm$  SEM. (G) Flow cytometry gating strategies to identify ChP fluorescent MTX uptake. Nonviable cells were excluded based on 7-amino-actinomycin D (7AAD) staining. These gating strategies were used in main **Figure 2B** (LV ChP) and **Figure S2A** (4V ChP). FSC-A, forward scatter area; SSC-A, side scatter area. (H) Flow cytometry gating strategies to identify mitochondrial membrane potential following ChP MTX treatment using MitoTracker Deep Red. These gating strategies were used in main **Figure 2D** (LV ChP) and **Figure S2C** (4V ChP). (I) Flow cytometry gating strategies to identify ROS production following ChP MTX treatment using CellROX. Nonviable cells were excluded based on 7AAD staining. These gating strategies were used in main **Figure 2F** (LV ChP) and **Figure S2E** (4V ChP).

### Supplemental Figure S3



**Supplemental Figure S3. ChP *Sod3* expression, Related to Figure 3.**

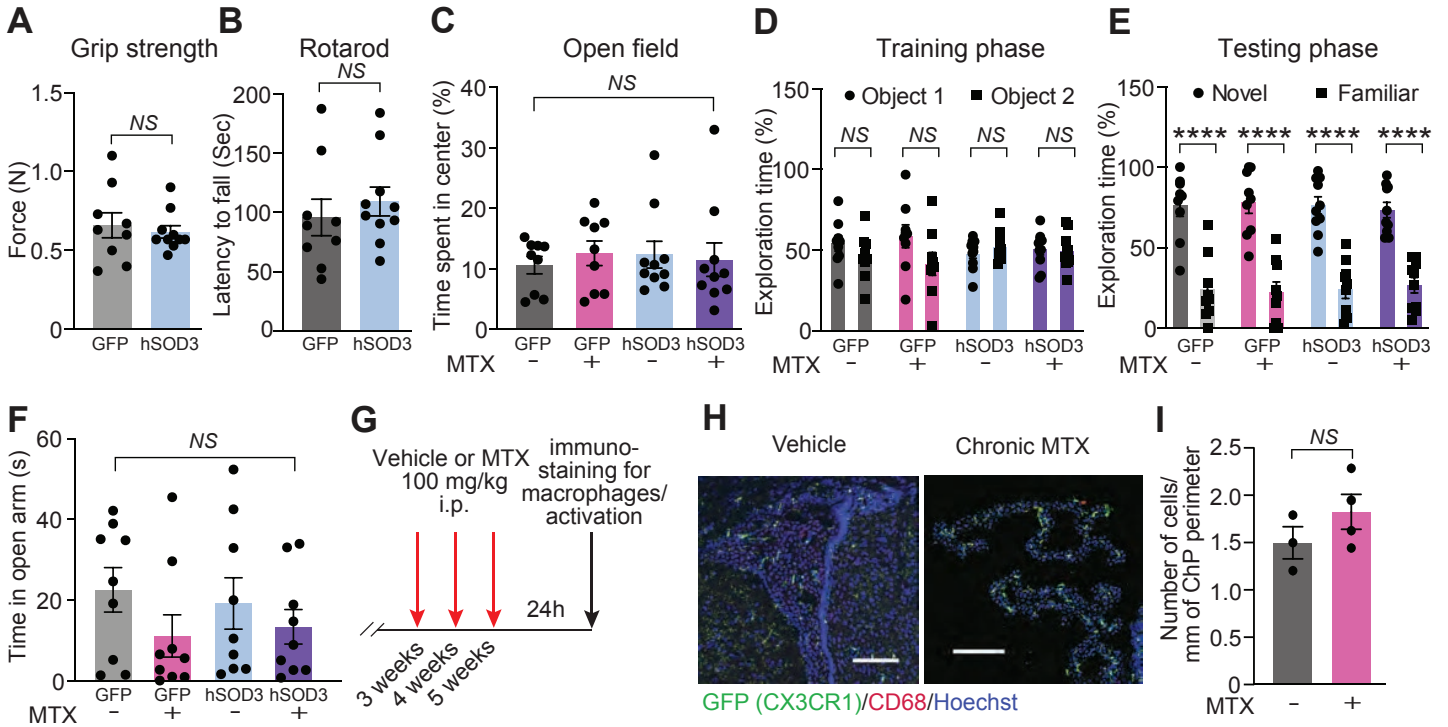
(A) t-SNE of *Sod3* expression in E16.5 ChP cell types (Dani et al., Cell 2021). (B) t-SNE showing *Sod3* expression in LV, 3V, and 4V ChP at E16.5 (Dani et al., Cell 2021).



**Supplemental Figure S4. Metabolic effect of exogenous SOD3 expression in ChP following MTX treatment and preconditioning oxidative stress of the CSF by the AAV-GFP overexpression system, Related to Figure 4.** (A) Representative LV ChP whole mount revealing location of sustained GFP expression (resulting from AAV-GFP transduction) near free margin of larger domain at 9 weeks and (B) 6 months. (C) Schematic of LV ChP whole mount depicting location of most prominent and long-lasting transduction of ChP epithelial cells in our paradigm (see also **Figure 4B**). (D) hSOD3 expression measured by qRT-PCR in the LV ChP and 4V ChP of mice transduced with AAV-hSOD3 and treated with either vehicle or 75 mg/kg MTX for 48 h. n = 4 per group. NS, not significant. Unpaired *t* test. Data represent mean  $\pm$  SEM. (E) Metabolite profiling of CSF samples from mice transduced with AAV-GFP or sham controls and treated with MTX as indicated. Heatmap of top 25 changed metabolites in the CSF is shown. The heatmap represents log-transformed, Pareto-scaled levels of each of the listed metabolites in the four conditions. (F) As in (E) but PLSDA loading plot and associated features driving group separation by indicated components are shown. (G) Relative levels of lysine, isoleucine, and lactic acid for indicated conditions upon MTX treatment. NS, not significant. Data represent mean  $\pm$  SEM.



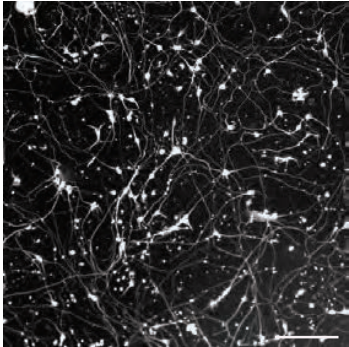
**Supplemental Figure S5**



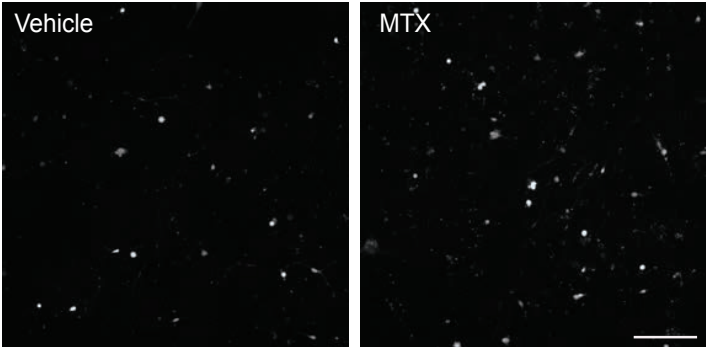
**Supplemental Figure S5. Behavior analyses and evaluation of inflammation in MTX-treated mice, Related to Figure 5.** (A-C) AAV-GFP and AAV-SOD3-treated mice showed no differences in (A) grip strength (n = 9 [male = 5, female = 4] AAV-GFP, n = 10 [male = 5, female = 5] AAV-hSOD3; NS, not significant, unpaired *t* test, data represent mean  $\pm$  SEM), (B) latency to fall on the accelerating rotarod (n = 9 [male = 5, female = 4] AAV-GFP, n = 10 [male = 5, female = 5] AAV-hSOD3; NS, not significant, unpaired *t* test, data represent mean  $\pm$  SEM), or (C) time exploring during the open field test (n = 9 [male = 5, female = 4] GFP + vehicle, n = 9 [male = 4, female = 5] GFP + MTX, n = 10 [male = 5, female = 5] SOD3 + vehicle, n = 10 [male = 5, female = 5] SOD3 + MTX; NS, not significant, one-way ANOVA with Tukey's post hoc test, data represent mean  $\pm$  SEM). (D-E) No differences were observed in the novel object recognition test in mice prophylactically treated with AAV-GFP or AAV-SOD3 during the training phase (D) or testing phase (E) (n = 9 [male = 5, female = 4] GFP + vehicle, n = 9 [male = 4, female = 5] GFP + MTX, n = 10 [male = 5, female = 5] SOD3 + vehicle, n = 10 [male = 5, female = 5] SOD3 + MTX; \*\*\*\**P* < 0.0001, NS, not significant, two-way ANOVA with Bonferroni's post hoc test, data represent mean  $\pm$  SEM). (F) No differences were observed in time spent in the open arm of the elevated plus maze in mice prophylactically treated with AAV-GFP or AAV-SOD3 and subsequently exposed to MTX (n = 9 [male = 5, female = 4] GFP + vehicle, n = 9 [male = 5, female = 4] GFP + MTX, n = 9 [male = 4, female = 5] SOD3 + vehicle, n = 9 [male = 4, female = 5] SOD3 + MTX; NS, not significant, one-way ANOVA with Bonferroni's post hoc test, data represent mean  $\pm$  SEM). (G) Experimental overview for evaluating ChP inflammation in the chronic MTX paradigm. (H) Representative images of LV ChP from *Cx3cr1-GFP<sup>+/-</sup>* mice stained with anti-GFP (macrophages, green) and CD68 (activated macrophages, red) antibodies and counterstained with Hoechst (nuclei, blue). (I) Quantification of macrophages identified in (H) per mm ChP (saline = 1.498  $\pm$  0.1699

macrophages per mm ChP,  $n = 3$ ; MTX =  $1.825 \pm 0.1850$  macrophages per mm ChP,  $n = 4$  per group. NS, not significant. Unpaired  $t$  test. Data represent mean  $\pm$  SEM.

**A** Baseline human cortical neuron



**B** CellROX spot intensity images



**Supplemental Figure S6. Human cortical neurons respond to MTX, Related to Figure 6.**

(A) Representative image of induced human cortical neuron cultures. (B) Representative CellROX spot intensity images of cultures prepared as in (A), treated with MTX (10  $\mu$ M) or vehicle for 72 h, and quantified in main **Figure 6A**. Scale bar, 200  $\mu$ m.



**Table S2. Clinical information of disease-free controls, Related to STAR Methods.**

<b>Case ID</b>	<b>Diagnosis</b>	<b>CSF collection Date</b>
<b>N1</b>	Headache	2011-09-13
<b>N2</b>	Facial numbness	2011-05-17
<b>N3</b>	Headache	2012-01-20
<b>N4</b>	Headache	2013-02-07
<b>N5</b>	Migraine	2015-03-24
<b>N6</b>	Headache	2018-10-02
<b>N7</b>	Pseudotumor cerebri	2018-10-19
<b>N8</b>	Degenerative spine disease	2019-04-17
<b>N9</b>	Progressive supranuclear palsy	2019-05-03
<b>N10</b>	Dementia	2020-12-02
<b>N11</b>	Bone cyst	2004-11-24
<b>N12</b>	Attention deficit	2008-01-10